REPORT DOCUMENTATION PAGE

OMB No. 0704-0188

AD-A238 413

Public reporting burden for this collection of information is estimated to average 1 hour per response, including the time for reviewing instructions, searching existing data sources, gathering and maintaining the data needed, and completing and reviewing the collection of information. Send comments regarding this burden estimate or any other aspect of this collection of information, including suggestions for reducing this burden, to Washington Headquarters Services, Directorate for information Operations and Reports, 1215 Jefferson Davis Highway, Suite 1204, Arlington, VA 22202-4302, and to the Office of Management and Budget, Paperwork Reduction Project (0704-0188), Washington, DC 20503.

TE	3. REPORT TYPE AND DATES COVERED
	Reprint 1991

Raman scattering of chromium-doped halide elpasolite crystals

5. FUNDING NUMBERS

DAAL03 86-K-0017

6. AUTHOR(S)

U. Sliwczuk, R.H. Bartram, D.R. Gabbe and B.C. McCollum

DTIC

7. PERFORMING ORGANIZATION NAME(S) AND ADDRESS(ES)

Department of Physics U-46
University of Connecticut
2152 Hillside Road
Storrs, CT 06269-3046

8. PERFORMING ORGANIZATION REPORT NUMBER

9. SPONSORING/MONITORING AGENCY NAME(S) AND ADDRESS(ES)

U. S. Army Research Office
P. O. Box 12211
Research Triangle Park, NC 27709-2211

10. SPONSORING/MONITORING AGENCY REPORT NUMBER

ARO 23118.7-PH

11. SUPPLEMENTARY NOTES

The view, opinions and/or findings contained in this report are those of the author(s) and should not be construed as an official Department of the Army position, policy, or decision, unless so designated by other documentation.

12a. DISTRIBUTION/AVAILABILITY STATEMENT

Approved for public release; distribution unlimited.

12b. DISTRIBUTION CODE

13. ABSTRACT (*Maximum 200 words*)

Abstract—Polarized Raman spectra of a single crystal of the chromium-doped elpasolite $K_2NaScF_6:Cr^{3+}$ yield an unambiguous identification of the symmetries and frequencies of the four Raman-active modes: a_{1g} at 525 cm^{-1}, e_g at 403 cm^{-1} and t_{2g} at 250 and 113 cm^{-1}. Low temperature spectra reveal a lower symmetry phase involving substantial distortion of the potassium sublattice. The impurity concentration dependence reveals a local mode of a_{1g} symmetry at 541 cm^{-1}. Vibration frequencies inferred from unpolarized Raman spectra are reported for a number of other halide elpasolites doped with either chromium or titanium.

14. SUBJECT TERMS	15. NUMBER OF PAGES
Raman scattering, elpasolite, chromium, phase transition, phonons	16. PRICE CODE

17. SECURITY CLASSIFICATION OF REPORT	18. SECURITY CLASSIFICATION OF THIS PAGE	19. SECURITY CLASSIFICATION OF ABSTRACT	20. LIMITATION OF ABSTRACT
UNCLASSIFIED	UNCLASSIFIED	UNCLASSIFIED	UL

NSN 7540-01-280-5500

Standard Form 298 (Rev 2-89)
Prescribed by ANSI Std 239-18
298-102

91-05522

J. Phys. Chem. Solids Vol. 52, No. 2, pp. 357–361, 1991
Printed in Great Britain.

0022-3697/91 $3.00 + 0.00
Pergamon Press plc

RAMAN SCATTERING OF CHROMIUM-DOPED HALIDE ELPASOLITE CRYSTALS

U. SLIWCZUK,† R. H. BARTRAM,† D. R. GABBE‡ and B. C. MCCOLLUM§

†Department of Physics and Institute of Materials Science, University of Connecticut, Storrs, CT 06269-3046, U.S.A.

‡Crystal Physics and Optical Electronics Laboratory, Massachusetts Institute of Technology, Cambridge, MA 02139, U.S.A.

§GTE Laboratories, Inc., 40 Sylvan Road, Waltham, MA 02154, U.S.A.

(*Received* 23 *July* 1990; *accepted* 14 *August* 1990)

Abstract—Polarized Raman spectra of a single crystal of the chromium-doped elpasolite $K_2NaScF_6:Cr^{3+}$ yield an unambiguous identification of the symmetries and frequencies of the four Raman-active modes: a_{1g} at 525 cm^{-1}, e_g at 403 cm^{-1} and t_{2g} at 250 and 113 cm^{-1}. Low temperature spectra reveal a lower symmetry phase involving substantial distortion of the potassium sublattice. The impurity concentration dependence reveals a local mode of a_{1g} symmetry at 541 cm^{-1}. Vibration frequencies inferred from unpolarized Raman spectra are reported for a number of other halide elpasolites doped with either chromium or titanium.

Keywords: Raman scattering, elpasolite, chromium, phase transition, phonons.

1. INTRODUCTION

The cubic elpasolite crystal structure with space group O_h^5 is consistent with first-order Raman scattering, in contrast to the perovskite structure from which it is derived. Raman spectra have been reported previously for both oxide elpasolites [1, 2] and halide elpasolites [3–11]. Of particular interest are those halide elpasolites with relatively large trivalent cations which exhibit a low temperature phase transition, exemplified by $Cs_2NaLnCl_6$, where Ln denotes a light trivalent rare-earth ion.

We have employed polarized Raman spectroscopy to investigate the dependence of normal-mode frequencies on temperature, impurity concentration and composition in a series of additional halide compounds of elpasolite structure. The materials investigated here, which were all prepared originally as potential tunable solid-state-laser materials, are intentionally doped with transition-metal impurities, mostly chromium. The optical absorption and emission spectra of chromium-doped halide elpasolites have been the objects of extensive investigation [12–24].

Raman-active normal modes of elpasolite are identified in Section 2, experimental methods are described in Section 3 and experimental results are presented in Section 4 and interpreted in Section 5.

2. IDENTIFICATION OF RAMAN-ACTIVE NORMAL MODES

The cubic elpasolite crystal structure is derived from the perovskite structure by alternate substitution of monovalent and trivalent cations on the divalent cation sublattice. The resulting compound has the formula A_2BMX_6, where A and B are monovalent cations, M is a trivalent cation and X is a monovalent anion. (This description applies to halide elpasolites; all of the charges are doubled in the oxide elpasolites.) The substitution of B and M for D in the perovskite ADX_3 removes the inversion symmetry at the sites of ions A and X, with the consequence that first-order Raman scattering, which is forbidden by inversion symmetry at all ion sites in perovskite, becomes allowed in elpasolite.

Only zone-center optical modes (approximately zero wave vector) of a_{1g}, e_g and t_{2g} symmetry are Raman active [25]. The elpasolite structure is face-centered cubic and the primitive unit cell comprises one formula unit of 10 ions. Of the 27 zone-center optical normal modes [26], just nine are Raman active with only four distinct vibration frequencies by virtue of symmetry-induced degeneracies. The corresponding symmetry-adapted displacements are illustrated in Fig. 1. The normal modes of t_{2g} symmetry are linear combinations of the symmetry-adapted displacements shown. However, since the anion X is much less massive than the cation A in the compounds investigated, the anion displacement is expected to predominate in the higher frequency t_{2g} mode, and the cation displacement in the lower. Since the higher frequency t_{2g} mode is primarily a bending mode, its frequency is expected to lie lower than that of the asymmetric e_g stretching mode, which in turn should lie below that of the symmetric a_{1g} stretching mode.

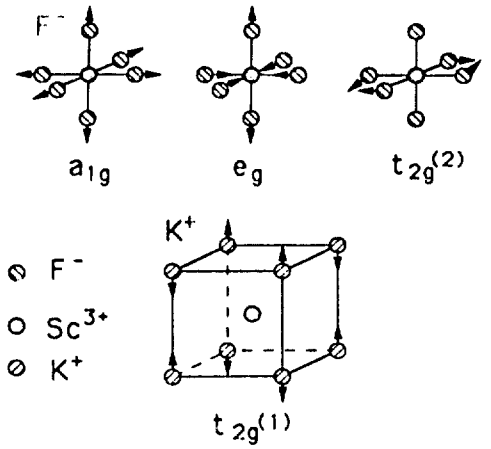

Fig. 1. Raman-active zone-center modes of the elpasolite K_2NaScF_6.

3. EXPERIMENTAL METHODS

The 5145 Å line of a Spectra-Physics 2025-05 argon-ion laser was used as the excitation source in our measurements, together with a narrow-band laser line filter to suppress Ar plasma lines. Scattered light was detected at 90° with respect to the direction of the incident light. Sheet polarizers were employed, and the scattered light was subsequently passed through a polarization scrambler into a computer controlled Spex double spectrometer (Spex 1404), equipped with 1800 lines mm^{-1} holographic gratings. Conventional photon counting techniques, including a low-noise photomultiplier (RCA 31034), preamplifier and amplifier/threshold discriminator, were employed for signal detection. The data were recorded and stored by an Apple IIe computer. The signal intensity was normalized to the exciting laser intensity.

Polarized Raman measurements were made on a single crystal of K_2NaScF_6 which was grown at MIT in a closed vessel by the Czochralski method with a Cr^{3+} doping of 1 at.%. Single crystals of $Cs_2NaInCl_6:Cr^{3+}$ and $Rb_2NaScF_6:Ti^{3+}$, both with nominal 1% doping, were also grown at MIT. The remaining samples employed in this investigation were small pieces of a variety of compounds with elpasolite structure selected from polycrystalline materials prepared at GTE Laboratories by slow cooling from the melt in sealed quartz or platinum tubes [20]. Two samples were doped with Cr^{3+} at 5 at.% and all of the remaining samples at 1%.

The single crystal of $K_2NaScF_6:Cr^{3+}$ was X-ray oriented and polished, and mounted on the cold finger of a Helitran flow-cryostat in two different orientations, as shown in Figs 2(a) and 2(b). In the orientation of Fig. 2(a), [001]→[100], polarization selection rules [25] dictate that light scattered by modes of a_{1g} and e_g symmetry is polarized parallel to the laser (∥) and is therefore observable only in $X(ZZ)Y$ scattering geometry, while light scattered by modes of t_{2g} symmetry is polarized perpendicular to the laser (⊥) and it is observable only in $X(ZX)Y$ geometry. In the orientation of Fig. 2(b), [011]→[100], light scattered by an e_g mode is predominantly polarized perpendicular to the laser (⊥); it is more intense by a factor of three in $X(ZX)Y$ geometry than in $X(ZZ)Y$ geometry. On the other hand, light scattered by both a_{1g} and t_{2g} modes is polarized parallel to the laser (∥) in this orientation and is thus observable only in $X(ZZ)Y$ geometry. Taken together, polarized Raman measurements in these two orientations suffice to distinguish all three allowed symmetries of Raman-active modes.

4. EXPERIMENTAL RESULTS

Polarized Raman spectra obtained at room temperature with a single crystal of $K_2NaScF_6:Cr^{3+}$ are shown in Figs 3 and 4 for the two sample orientations of Fig. 2. Two scattering geometries are employed for each orientation, $X(ZZ)Y$ and $X(ZX)Y$, yielding spectra polarized parallel (∥) and perpendicular (⊥) to the laser, respectively. These four spectra, together with the polarization selection rules listed above, suffice to provide a unique determination of the symmetry of each Raman-active mode. There are four principal lines as expected, and they appear in the anticipated order ($t_{2g}^{(1)}$, $t_{2g}^{(2)}$, e_g and a_{1g} with increasing frequency); thus the lines can be confidently correlated with the symmetry-adapted displacements shown in Fig. 1.

It is evident from Fig. 5 that pronounced qualitative changes in the Raman spectra are observed at liquid nitrogen temperature. Two distinct novel features are evident: (1) a splitting of the $t_{2g}^{(1)}$ line into several lines; and (2) the appearance of side structure associated with the a_{1g} line. The origins of these two features appear to be quite different. The splitting of the $t_{2g}^{(1)}$ line develops continuously with diminishing temperature, as shown in Fig. 6, suggesting that it is associated with a phase transition. The side structure of the a_{1g} line, on the other hand, is simply seen with better resolution at low temperature. A comparison of the Raman spectra of $K_2NaScF_6:Cr^{3+}$ samples

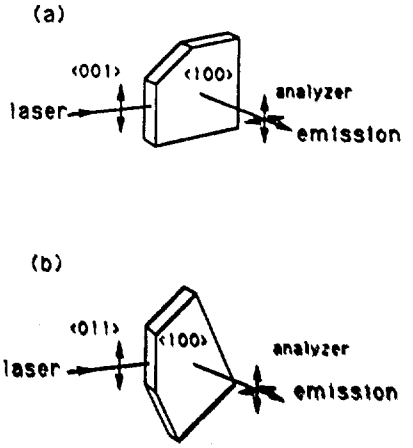

Fig. 2. Two orientations of the $K_2NaScF_6:Cr^{3+}$ single crystal employed in polarized Raman scattering measurements.

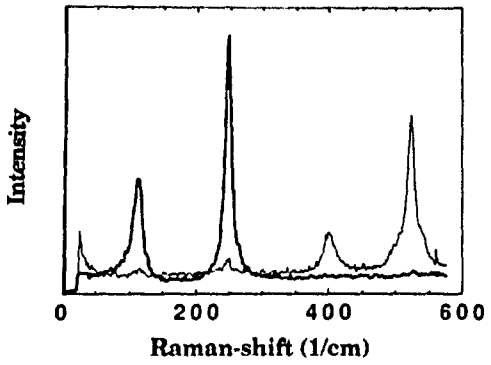

Fig. 3. Polarized room-temperature Raman spectra of $K_2NaScF_6:Cr^{3+}$ (1%) for sample orientation (a) of Fig. 2, with parallel (– – –) and perpendicular (———) polarizations.

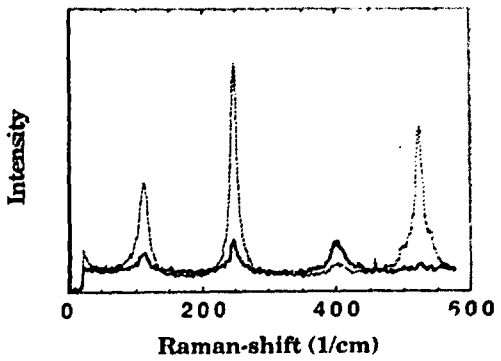

Fig. 4. Polarized room-temperature Raman spectra of $K_2NaScF_6:Cr^{3+}$ (1%) for sample orientation (b) of Fig. 2, with parallel (– – –) and perpendicular (———) polarizations.

with 1 and 5% impurity concentrations, shown in Fig. 7, reveals that this side structure is impurity related.

Unpolarized, room-temperature Raman spectra have been obtained on a number of elpasolite crystals doped with chromium or, in one case, titanium. The phonon energies for vibrations of the host lattice are listed in Table 1; the modes are identified by analogy with those of K_2NaScF_6.

5. DISCUSSION

The four principal lines observed in the first-order Raman spectrum of $K_2NaScF_6:Cr^{3+}$ are attributed to the zone-center normal modes of the host crystal. The symmetry of the mode corresponding to each line has been identified unambiguously by polarized Raman spectroscopy, and the lines appear in the anticipated order of vibration frequency. Host-lattice vibration frequencies are reported here for a number of additional halide compounds of elpasolite structure, as well.

The splitting of the $t_{2g}^{(1)}$ line in $K_2NaScF_6:Cr^{3+}$ is attributed to a phase transition which occurs at room temperature. The fact that only the $t_{2g}^{(1)}$ line is appreciably affected suggests that the phase transition involves relatively little distortion of the $(ScF_6)^{3-}$ octahedral complexes. It may well be that the room-temperature phase transition is initiated by a soft t_{1g} librational mode of the $(ScF_6)^{3-}$ octahedra, as in the $Cs_2NaLnCl_6$ system; such a mode is invisible to Raman scattering. The consequent reduction to tetragonal symmetry could account for the splitting of the $t_{2g}^{(1)}$ line observed at 225 K, as shown in Fig. 6.

Additional distortion of the potassium sublattice is observed at still lower temperatures. Of particular interest is the lowest energy line in Fig. 6 which appears to move in from the laser line as the temperature is reduced. This line may correspond to a Raman-active soft mode associated with a second phase transition, as has been reported in the analogous compound $Cs_2LiCr(CN)_6$ [27]. From its polarization dependence, it appears to be a composite of two lines. The presence of at least seven lines with frequencies below 140 cm^{-1} at 90 K suggests a distortion which not only removes the degeneracy of Raman-active modes but also enlarges the primitive unit cell, thus introducing additional zone-center Raman-active modes. Little additional change is observed in the spectrum as the temperature is reduced to 10 K.

The side structure of the a_{1g} lines, whose resolution is enhanced at low temperature, is attributed to local and resonance modes associated with the Cr^{3+} impurities. This interpretation is corroborated by the concentration dependence of the Raman spectrum shown in Fig. 7. The elpasolite crystal structure has the property that it can accommodate a trivalent cation substitutional impurity at a site of rigorously octahedral symmetry without charge compensation. Thus the point symmetry is unaffected by doping and only the translational symmetry is lost.

Table 1. Phonon energies (cm^{-1}) of Raman-active modes of vibration in some transition-metal-doped halide elpasolites

Crystal	Doping (%)	$t_{2g}^{(1)}$	$t_{2g}^{(2)}$	e_g	a_{1g}
$K_2NaScF_6:Cr^{3+}$	5	115	251	409	525
$K_2NaScF_6:Cr^{3+}$	1	113	250	403	525
$K_2NaGaF_6:Cr^{3+}$	1	124	284	—	553
$K_2LiScF_6:Cr^{3+}$	1	113	265	378	527
$Rb_2NaScF_6:Ti^{3+}$	1	87	244	388	512
$Cs_2NaInCl_6:Cr^{3+}$	1	50	142	—	294
$Cs_2NaYCl_6:Cr^{3+}$	1	47	127	222	284
$Cs_2NaYCl_6:Cr^{3+}$	1	46	127	223	284
$Cs_2NaScCl_6:Cr^{3+}$	1	51	148	205	290

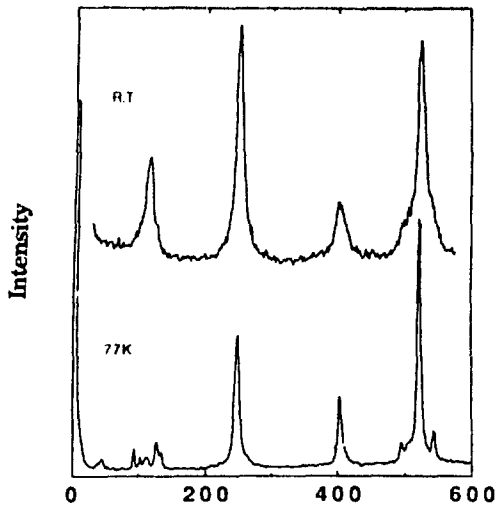

Fig. 5. Comparison of unpolarized Raman spectra of $K_2NaScF_6:Cr^{3+}$ (1%) at room temperature and at 77 K.

quently, the polarization selection rules are preserved but not the restriction to zone-center phonons. It is clear from its polarization behavior that all of the side structure is associated with the projected density of states for perturbed a_{1g} vibrations. In particular, the relatively narrow line at 541 cm^{-1} lies above all the vibriation frequencies of the perfect lattice and is therefore associated with a true local mode.

It is evident from Fig. 7 that the integrated intensity of the a_{1g} side structure with 5% chromium concentration is comparable with that of the a_{1g} host-lattice line; however, no side structure is observed in association with host-lattice lines of other symmetries. An obvious inference is that the a_{1g} mode

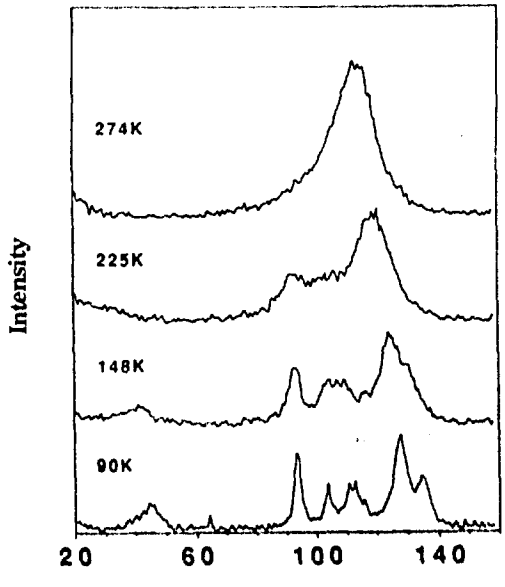

Fig. 6. Temperature dependence of the expanded low-frequency portion of the unpolarized Raman spectrum of $K_2NaScF_6:Cr^{3+}$ (1%).

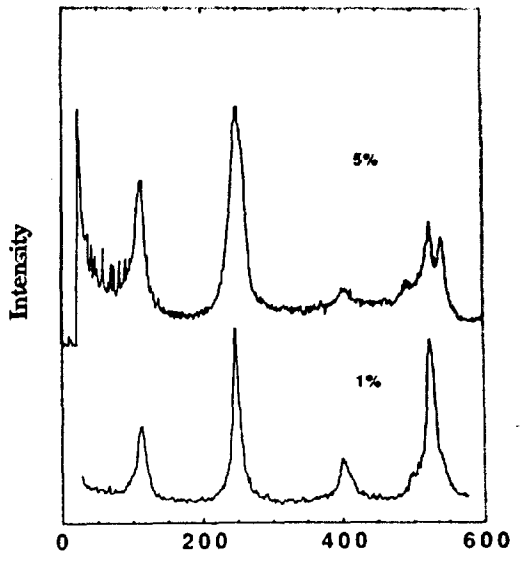

Fig. 7. Chromium concentration dependence of the unpolarized room-temperature Raman spectrum of $K_2NaScF_6:Cr^{3+}$.

localized at the chromium impurity has an unusually large Raman cross-section.

Acknowledgements—This work was supported by the U.S. Army Research Office under Contract No. DAAL03-86-K-0017. The authors are grateful to Drs H. Jenssen, D. S. Hamilton and L. J. Andrews for advice and assistance.

REFERENCES

1. Lentz A., *Z. anorg. allg. Chem.* **392**, 218 (1972).
2. Corsmit A. F., Hoefdraad H. E. and Blasse C., *J. inorg. nucl. Chem.* **34**, 3401 (1972).
3. Lentz A., *Z. anorg. allg. Chem.* **408**, 255 (1974).
4. Schwartz R. W., Watkins S. F., O'Connor C. J. and Carlin R. L., *J. chem. Soc. Faraday Trans.* II **72**, 565 (1976).
5. O'Connor C. J., Carlin R. L. and Schwartz R. W., *J. chem. Soc. Faraday Trans.* II **73**, 361 (1977).
6. Becker R., Lentz A. and Sawodny W., *Z. anorg. allg. Chem.* **420**, 210 (1976).
7. Amberger H.-D., Rosenbauer G. G. and Fischer R. D., *J. Phys. Chem. Solids* **38**, 379 (1977).
8. Nevald R., Voss F. W., Nielsen O. V., Amberger H.-D. and Fischer R. D., *Solid St. Commun.* **32**, 1223 (1979).
9. Knudsen G. P., Voss F. W., Newald R. and Amberger H.-D., in *The Rare Earths in Modern Science and Technology*, Vol. 3, pp. 335–338. Plenum Press, New York (1982).
10. Pelle F., Blanzat B. and Chevalier B., *Solid St. Commun.* **49**, 1089 (1984).
11. Selgert P., Lingner C. and Lüthi B., *Z. Phys. B Cond. Matter* **55**, 219 (1984).
12. Wood D. L., Ferguson J., Knox K. and Dillon J. F., Jr, *J. chem. Phys.* **39**, 890 (1963).
13. Schläefer H. L., Gausmann H. and Witzke H., *J. chem. Phys.* **46**, 1423 (1967).
14. Ferguson J., Guggenheim H. J. and Wood D. L., *J. chem. Phys.* **54**, 504 (1971).
15. Schwartz R. W., *Inorg. Chem.* **15**, 2817 (1976).
16. Güdel H. V. and Snellgrove T. R., *Inorg. Chem.* **17**, 1617 (1978).

17. Greenough P. and Paulusz A. G., *J. chem. Phys.* **70,** 1967 (1979).
18. Kenyon P. T., Andrews L., McCollum B. and Lempicki A., *IEEE J. Quantum Electron.* **QE-18,** 1189 (1982).
19. Dolan J. F., Kappers L. A. and Bartram R. H., *Phys. Rev.* **B33,** 7339 (1986).
20. Andrews L. J., Lempicki A., McCollum B. C., Giunta C. J., Bartram R. H. and Dolan J. F., *Phys. Rev.* **B34,** 2735 (1986).
21. Bartram R. H., Charpie J. C., Andrews L. J. and Lempicki A., *Phys. Rev.* **B34,** 2741 (1986).
22. Andrews L. J., Hitelman S. M., Kokta M. and Gabbe D., *J. chem. Phys.* **84,** 5229 (1986).
23. Knochenmuss R., Reber C., Rajasekharan M. V. and Güdel H. V., *J. chem. Phys.* **85,** 4280 (1986).
24. Bartram R. H., Dolan J. F., Charpie J. C., Rinzler A. G. and Kappers L. A., *Cryst. Latt. Def. amorph. Mater.* **15,** 165 (1987).
25. Hayes W. and Loudon R., *Scattering of Light by Crystals.* Wiley, New York (1978).
26. Lentz A., *J. Phys. Chem. Solids* **35,** 827 (1974).
27. Ryan R. R. and Swanson B. I., *Phys. Rev.* **B13,** 5320 (1976).

Accession For
NTIS GRA&I
DTIC TAB
Unannounced
Justification
By
Distribution/
Availability Codes
Dist | Avail and/or Special
A-1 | 20

END

FILMED

DATE: 7-91

DTIC